

VLA 8.4-GHz monitoring observations of the CLASS gravitational lens B1933+503

A. D. Biggs,¹ E. Xanthopoulos,¹ I. W. A. Browne,¹ L. V. E. Koopmans² and C. D. Fassnacht³

¹*University of Manchester, Jodrell Bank Observatory, Macclesfield, Cheshire SK11 9DL*

²*University of Groningen, Kapteyn Astronomical Institute, Postbus 800, 9700 AV Groningen, the Netherlands*

³*National Radio Astronomy Observatory, PO Box 0, Socorro, NM 87801, USA*

Accepted . Received

ABSTRACT

The complex ten-component gravitational lens system B1933+503 has been monitored with the VLA during the period February to June 1998 with a view to measuring the time delay between the four compact components and hence to determine the Hubble parameter H_0 . Here we present the results of an ‘A’ configuration 8.4-GHz monitoring campaign which consists of 37 epochs with an average spacing of 2.8 days. The data have yielded light curves for the four flat-spectrum radio components (components 1, 3, 4 and 6). We observe only small flux density changes in the four flat-spectrum components which we do not believe are predominantly intrinsic to the source. Therefore the variations do not allow us to determine the independent time delays in this system. However, the data do allow us to accurately determine the flux density ratios between the four flat-spectrum components. These will prove important as modelling constraints and could prove crucial in future monitoring observations should these data show only a monotonic increase or decrease in the flux densities of the flat-spectrum components.

Key words: galaxies: individual: B1933+503 – cosmology: observations – gravitational lensing

1 INTRODUCTION

B1933+503 is the most complex arcsec-scale gravitational lens system known and the most noteworthy system discovered in the Cosmic Lens All-Sky Survey (CLASS; Browne et al. 1998), a survey of approximately 15,000 flat-spectrum radio sources observed with the VLA at 8.4 GHz with a resolution of 200 milliarcsec (mas). Sykes et al. (1998) report the discovery of this lens and present VLA and MERLIN maps that reveal up to ten components, four of which are compact and have flat spectra while the rest are more extended and have steep spectra. The ten components are believed to be the multiple images of a background source that consists of a flat-spectrum core (quadruply imaged) and two compact lobes symmetrically situated on opposite sides of the core (one quadruply imaged and the other doubly imaged). A *Hubble Space Telescope* (HST)/WFPC2 image (*I*-band) of B1933+503 (Sykes et al. 1998) shows a faint galaxy with a compact core (the lensing galaxy) but none of the images of the background object are detected. Spectra taken with the Keck telescope have given a redshift for the lensing galaxy of 0.755 (Sykes et al. 1998). Sub-mm observations

of B1933+503 (Chapman et al. 1998) pointed to the fact that the source of the lens system should be lying above a redshift of 2 and that has been confirmed recently by observations made with the United Kingdom Infra-red Telescope (UKIRT) that have yielded a redshift of 2.62 for the background source (Norbury et al., in preparation).

HST NICMOS F160W-band observations (Marlow et al. 1998) of B1933+503 have uncovered the infra-red counterparts to two of the four compact components. These same two components were also detected in a VLBA 1.7-GHz map with a resolution of 6 mas. Marlow et al. suggest that the failure to detect the other two flat-spectrum components in the infra-red can be due to either rapid variability on a time-scale less than the time delay or due to extinction in the interstellar medium (ISM) of the lensing galaxy. The absence of these same two components in the radio could arise due to scatter-broadening of the images when propagating through the ISM of the lens galaxy as well as from time variability.

B1933+503 offers a unique opportunity to construct an accurate mass model due to the wealth of observational con-

straints that are available. As well as the large number of images, yielding both positional and flux density ratio constraints, some of these are extended. Perhaps more crucial is that three epochs of VLA 15-GHz data (Sykes et al. 1998) suggest that the flat-spectrum components are variable, by as much as 33 per cent over the period July to September 1995. This means that it should be possible to determine the relative time delays from flux density monitoring. Taken together this makes B1933+503 a promising system for a determination of the Hubble constant, H_0 (Refsdal 1964). The observational constraints given by Sykes et al. (1998) have been used as a starting point for the model presented by Nair (1998). The time delays of the flat-spectrum components with respect to component 1 derived from this model are approximately 8 d for component 3, 7 d for component 4 and 9 d for component 6.

In this paper we present the results of a four-month monitoring campaign using the VLA in its ‘A’ configuration at a frequency of 8.4 GHz. This frequency was chosen over 15 GHz (where the magnitude of flux density variations are likely to be greater) for a number of reasons. As well as the sensitivity of the VLA being greater at 8.4 GHz, the phase stability of the array is much poorer at 15 GHz. In addition, VLA 15-GHz monitoring of the lens system B0218+357 (Biggs et al. 1999) showed that at this frequency the data are subject to calibration errors of a few per cent due to the gains of the antennas varying with elevation. In Section 2 we describe the observations and observing strategy as well as the reduction methods that we used on the data. In Section 3 we show the light curves that were obtained from the data and we follow this with a discussion of the results.

2 OBSERVATIONS AND DATA REDUCTION

B1933+503 was observed between February 16 1998 and June 1 1998, during which time the VLA was in its ‘A’ configuration. The 37 epochs were separated, on average, by 2.8 d. The observations were made simultaneously in two frequency bands (IFs) each with a bandwidth of 50 MHz and centre frequencies of 8.4351 and 8.4851 GHz respectively. This gives an angular resolution of approximately 200 mas.

The observing strategy was kept as consistent as possible over the period of the monitoring. At each epoch the B1933+503 observations were split into two or three scans, each of approximately 6 min duration. Before and after each of the B1933+503 scans were separate (\sim one min duration) scans of the steep-spectrum source B1943+546 (Patnaik et al. 1992) which was used as the phase and amplitude calibrator. B1943+546 has all the requirements of a good primary calibrator being close to the target, having a strong correlated flux density and being relatively unresolved with the VLA at this frequency. The duration of the combined observations of both sources at a typical epoch was 30 min, but several epochs consisted of 20 min observing time.

Calibration was performed using the NRAO Astronomical Image Processing Software package AIPS and each IF was calibrated separately. The first step was to make the best possible map of 1943+546 as this calibrator is slightly resolved at the observing frequency. This was done by performing a first order calibration of several best epochs of 1943+546 data assuming the flux density of 610 mJy mea-

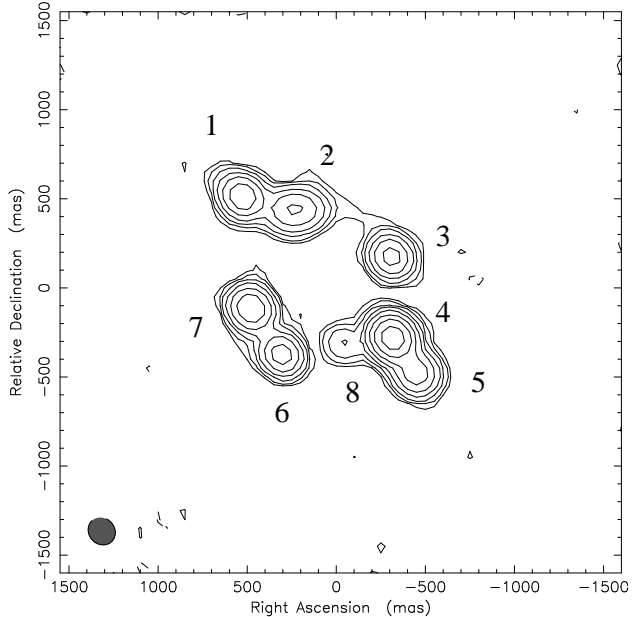


Figure 1. The VLA 8.4-GHz map of B1933+503 made from ten epochs of monitoring data. The map center is at RA 19 34 30.932 and DEC +50 25 23.502 (J2000 coordinates). The contours are equal to $-0.5, 0.5, 1, 2, 4, 8, 16, 32, 64$ per cent of the maximum value of $14.4 \text{ mJy beam}^{-1}$.

sured by Patnaik et al. (1992). This source has a steep spectrum and is found from VLBI maps (Polatidis et al. 1995; Xu et al. 1995) to be dominated by emission from two extended lobes on scales of ~ 50 pc. Therefore it is unlikely that the source’s flux density will have changed significantly since this measurement or that it will have changed over the period of the monitoring. These epochs were then combined and iteratively mapped and self-calibrated. The structure found from this map agrees well with that seen in the above mentioned VLBI maps. The CLEAN components from the map were then used as a model input to the AIPS task CALIB to derive telescope gain solutions at each epoch of observation. These gain solutions were then applied to the target B1933+503.

The positions and approximate flux densities of each component of B1933+503 were first established by making a map of the source. In order to make a high dynamic-range map of the source we combined ten epochs of observations with the DBCON task. As the images of the radio core are seen in higher resolution MERLIN maps to be compact, a traditional CLEAN was not used to make the map. Instead, a single delta component (point source) was placed at the approximate position of each of the compact components in the dirty map and the positions and flux densities of these were then optimised by model-fitting. Once the best fit had been found, the remaining extended flux was then CLEANed in the usual way. The resulting map is shown in Fig. 1 with eight of the ten components labelled. The remaining two components cannot be easily distinguished due to the low resolution of the image. Higher resolution observations and lens modelling have shown that component 2 actually consists of two merging images, denoted 2a and

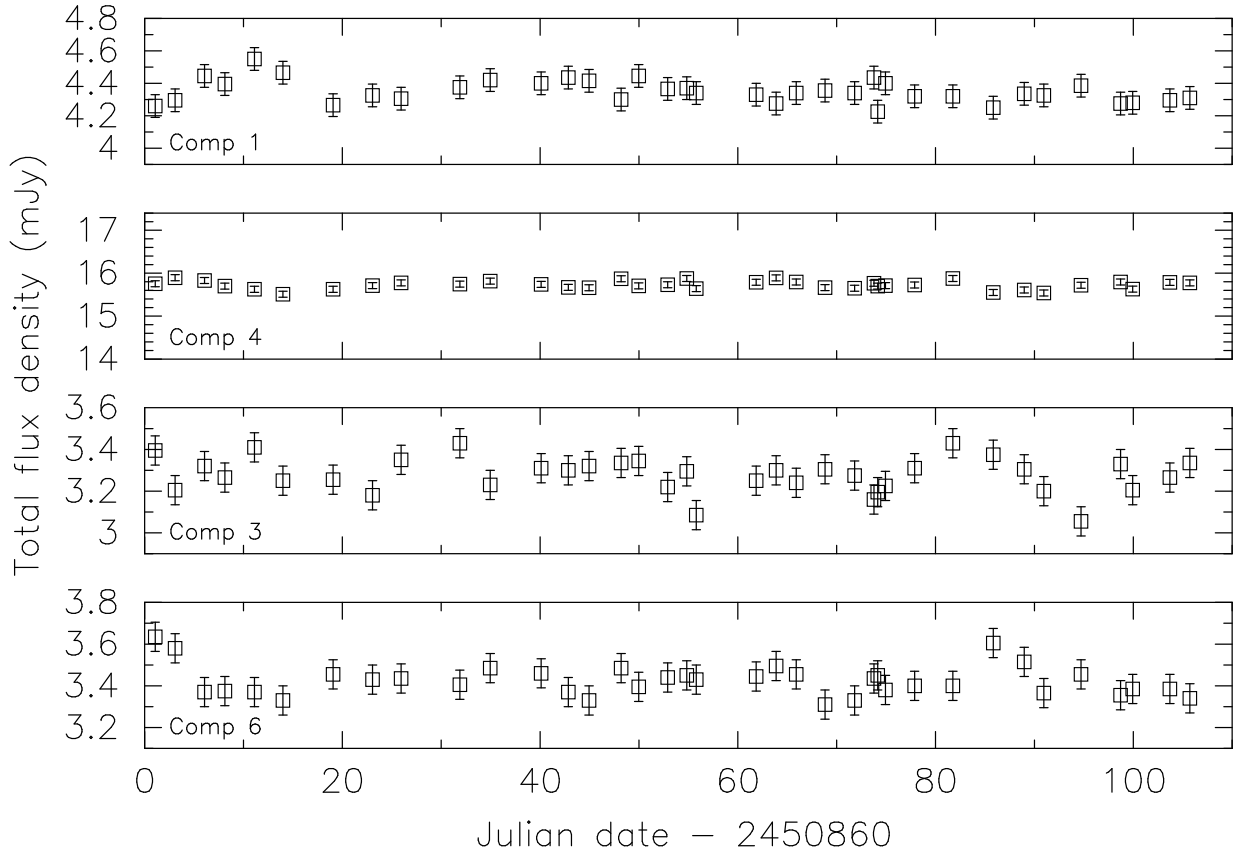


Figure 2. The 8.4 GHz total flux density light curves for the four flat-spectrum components of B1933+503. The components have been plotted in the order in which they are predicted to vary, beginning with component 1 at the top of the figure and followed by components 4, 3 and 6 respectively. The range along the y-axis has been set to a fixed fraction ($\sim 20\%$) of the average flux density for each component.

2b by Nair (1998). The remaining component (1a) can be barely discerned in Fig. 1 as a slight extension to the north-east of component 1. This extension is much more obvious in a MERLIN 1.7-GHz map (Sykes et al. 1998).

The flux densities of the four compact components of B1933+503 were determined by model-fitting directly to the (u, v) data, and to each IF individually, using the DIFMAP (Pearson et al. 1994; Shepherd 1997) model fitter. Each epoch of monitoring data was fit using the model derived from the map with all flux densities and positions held constant, except for the flux densities of the four compact components which were allowed to float. The model fit was interspersed with two iterations of phase self-calibration followed by a final overall amplitude correction i.e. one correction for each antenna for the entire observing period, normalising against the extended structure whose brightness should not vary over the monitoring observations. These amplitude corrections are never more than a few per cent per telescope. The reduced χ^2 indicated a reasonably good fit to each epoch, with a mean value of 1.35 and an rms scatter of 0.04 for each IF's data. At this point the two flux density measurements at each epoch from each IF are averaged together.

3 RESULTS

The averaged total flux density light curves for components 1, 4, 3 and 6 are shown in Fig. 2 and are plotted from the top of the figure downwards in the order in which they are expected to vary. The range encompassed by the y-axis is, for each component, equal to the same fraction ($\sim 20\%$) of the average flux density calculated over the period of the monitoring. The error bars attached to each data point have been estimated from a consideration of the difference between the flux densities derived from each IF at each epoch. For each component, a frequency histogram of the flux density difference at each epoch is approximately Gaussian with a mean that does not differ from zero by more than 0.02 mJy. The 1σ error derived using this method for each component is very similar and has been fixed at 0.07 mJy in Figure 2. This is in fact only a lower limit to the uncertainty in the flux densities as it does not take into account errors that are correlated in each IF. These include errors arising from overall amplitude miscalibration and those that are a function of the (u, v) coverage of the data which is essentially the same for each IF of a given epoch.

From the variations seen in Figure 2 it does not appear that the source has varied significantly during the course of

Table 1. Flux densities of the flat-spectrum radio components at 8.4 GHz for three different epochs (from 1994, 1995 and 1998). Typical flux density errors are 0.4 mJy. Flux density ratios of components 3, 4 and 6 with respect to 1.

Component	Flux density (mJy)			Flux density ratio		
	8.4 GHz			8.4 GHz		
	(1994)	(1995)	(1998)	(1994)	(1995)	(1998)
1	4.6	4.3	4.3	1.00	1.00	1.00
3	3.5	3.4	3.3	0.76	0.79	0.77
4	17.6	15.7	15.7	3.83	3.65	3.65
6	3.8	3.6	3.4	0.83	0.83	0.79

our monitoring campaign. This conclusion is supported in a number of ways. First, the mean flux density and rms percentage scatter about this mean for components 1, 4, 3 and 6 are: 4.35 mJy, 15.73 mJy, 3.25 mJy and 3.43 mJy, and 1.6, 0.6, 2.6, and 2.2 per cent respectively. What is apparent is that the rms scatter in the light curves is inversely proportional to the mean flux density of the component. If there were actually a dominant signal of intrinsic variability then it would be expected that the fractional scatter in the data would be equal for each component. This is not the case. This can be seen most clearly by comparing the ‘variability’ seen in the brightest component (4) which is much less than that seen in the other three fainter components. Also, a preliminary time delay analysis using both a chi-squared minimisation and the Dispersion method of Pelt et al. (1996) result in best-fit time delays that are totally at odds with those predicted by lens models of this system. The rms scatters quoted above are in general larger than expected from thermal noise considerations alone (by factors of ~ 2 – 3) and indicate that the data are corrupted by errors stemming from deconvolution and model fitting. Errors introduced by incorrect amplitude calibration from epoch to epoch must be present at a low level ($\leq 0.6\%$) as these would produce the same fractional scatter in each component.

Table 1 lists the flux densities of the four flat-spectrum components measured from the map in Fig. 1 together with previous values obtained at 8.4 GHz with the VLA in ‘A’ configuration on July 6, 1995 (Sykes et al. 1998) as well as those determined from the original VLA snapshot observation taken in 1994. We see that although there were no changes between the two most recent epochs there are signs that the overall flux density of these compact components in 1994 was higher than that in the last two epochs. As flux density variability has been reported at 15 GHz by Sykes et al. (1998) and because a comparison of the MERLIN and VLA maps by the same authors support variations in the relative flux densities of the same components we think that this source has been, and will probably again be, variable.

4 CONCLUDING REMARKS

We have presented the results of a four month program of monitoring the ten-component lens system B1933+503 with the VLA which have not allowed us to measure the independent time delays in this otherwise promising system for determining H_0 . The component light curves show fluctuations of 0.7–2.5 per cent which we do not believe represent source variability. Instead they are more likely to result from a combination of thermal noise, deconvolution and model fit-

ting errors. Since the system has already shown indications of variability (Sykes et al. 1998), we think that we have caught this system in a quiescent phase. For this reason, we have embarked on a second monitoring campaign that commenced in June 1999, also with the VLA at 8.4 GHz. An advantage that we have now over the previous attempt is that the flux density ratios between the components are known to high accuracy. Since we did not detect any variability during the 4 month monitoring campaign, which is a period significantly longer than the predicted time delay of 7–9 d, we have determined the intrinsic flux density ratios (Table 1). Therefore, should this second set of observations again not show reliable features that can be identified in each light curve, but do show a monotonic increase or decrease in flux density, a time delay may still be determined. This has previously been demonstrated by Koopmans et al. (1999) for the CLASS lens B1600+434.

ACKNOWLEDGMENTS

This research was supported by European Commission, TMR Programme, Research Network Contract ERBFMRXCT96-0034 “CERES”. The VLA is operated by the National Radio Astronomy Observatory which is supported by the National Science Foundation operated under cooperative agreement by Associated Universities, Inc. ADB acknowledges the receipt of a PPARC studentship.

REFERENCES

- Biggs A. D., Browne I. W. A., Helbig P., Koopmans L. V. E., Wilkinson P. N., Perley R. A., 1999, MNRAS, 304, 349
- Browne, I. W. A. et al., 1998, in Bremer, M. N., Jackson, N., Pérez-Fournon, I., eds, *Observational Cosmology with the new radio surveys*, Astrophysics and Space Science Library, Vol. 226. Dordrecht: Kluwer Academic Publishers, p. 323
- Chapman, S. C., Scott, D., Lewis, G. F., Borys, C., Fahlman, G. G., 1998, astro-ph/9810444
- Koopmans, L. V. E., de Bruyn, A. G., Xanthopoulos, E., Fassnacht, C. D., 1999, A&A, submitted
- Marlow, D. R., Browne, I. W. A., Jackson, N. J., Wilkinson, P. N., 1998, MNRAS, 305, 15
- Nair, S., 1998, MNRAS, 301, 315
- Patnaik A. R., Browne I. W. A., Wilkinson P. N., Wrobel J. M., 1992, MNRAS, 254, 655
- Pearson, T. J., Shepherd, M. C., Taylor, G. B., Myers, S. T., 1994, BAAS 185, #08.08
- Pelt J., Kayser R., Refsdal S., Schramm T., 1996, A&A, 305, 97
- Polatidis, A. G., Wilkinson, P. N., Xu, W., Readhead, C. S., Pearson, Taylor, G. B., Vermeulen, R. C., 1995, ApJS, 98, 1
- Refsdal S., 1964, MNRAS, 128, 307

- Shepherd M. C., 1997, *Astron. Data. Anal. Software Syst.*, 6, 77
Sykes, C. M. et al., 1998, *MNRAS*, 301, 310
Xu, W., Readhead, C. S., Pearson, T. J., Polatidis, A. G., Wilkinson, P. N., 1995, *ApJS*, 99, 297